THE JOURNAL OF PHYSICAL CHEMISTRY B

Article

pubs.acs.org/JPCB

Proton Transfer Step in the Carbon Dioxide Capture by Monoethanol Amine: A Theoretical Study at the Molecular Level

Kenji Iida and Hirofumi Sato*

Department of Molecular Engineering, Kyoto University, Kyoto, 615-8510, Japan

ABSTRACT: An aqueous solution of monoethanol amine (MEA) has been utilized in an industrial process of CO_2 absorption. The chemical reaction between CO_2 and MEA, which is employed in the process, consists of two steps. After the formation of the MEA−CO_2 complex ("capture"), a proton transfers from the complex to give a final product. In the present study, the overall mechanism of the reaction is discussed, especially focusing on the proton transfer step. Using RISM-SCF-SEDD, a hybrid method of electronic structure theory and statistical mechanics for molecular liquid, we clarified that the role of MEA as a base is crucial in the proton transfer step.

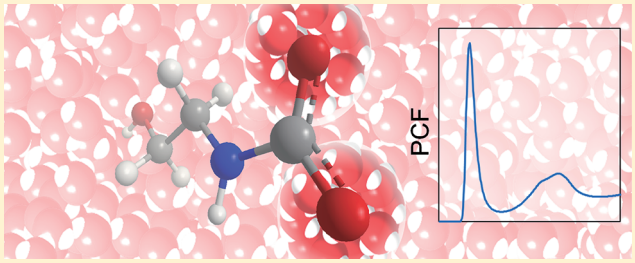

INTRODUCTION

In relation to global warming, chemical absorption of CO_2 by amine attracts much attention as the industrial process for CO_2 removal from flue gases. Monoethanolamine ($CH_2OHCH_2NH_2$; MEA) is one of the representative absorbents. Although MEA absorbs CO_2 sufficiently fast, the formed N−C bond is too strong to be broken under a mild condition. In other words, an excess amount of energy is necessary to reproduce MEA solution. A more efficient amine is thus highly desired, and the search for a new amine is extensively performed.

To find a more efficient amine, knowledge about the mechanism of CO_2 adsorption by MEA should be valuable. On the basis of experimental studies, it is known that two steps are involved in the process.[1−6] The first step is the bond formation between MEA (**1a**) and CO_2 (**1b**)

$$CH_2OHCH_2NH_2\ (\mathbf{1a}) + CO_2\ (\mathbf{1b}) \rightarrow CH_2OHCH_2NH_2{-}CO_2\ (\mathbf{3}) \quad (1)$$

Then a proton transfer occurs from the MEA−CO_2 complex (**3**) to a base (B)

$$CH_2OHCH_2NH_2{-}CO_2\ (\mathbf{3}) + B \rightarrow CH_2OHCH_2NHCOO^-\ (\mathbf{4}) + BH^+\ (\mathbf{5}) \quad (2)$$

Whereas step 1 is already established as the rate-determining step, step 2 is not fully understood. For example, it still remains an open question which MEA or H_2O acts as the base. Because the amount of required energy for reproducing MEA solution is mainly determined by the relative stability of the final products (**4** + **5**) to the reactants (**1a** + **1b**), it is essentially important to clarify the mechanism of step 2. Note that the solvation effect plays a central role in this reaction because it does not proceed in the gas phase. It is thus indispensable to treat both quantum chemistry and an ensemble of solvent molecules to grasp the essence of the reaction. RISM-SCF-SEDD[7−9] is a hybrid method of RISM theory[10,11] and ab initio molecular orbital theory. Different from QM/MM, which is a popular method to treat chemical reaction in the solution phase, RISM-SCF-SEDD utilizes RISM theory to treat solvent. The RISM theory is expressed as an algebraic equation in statistical mechanics for an ensemble of an infinite number of solvent molecules. With RISM-SCF-SEDD, we can obtain a wealth of knowledge about the electronic structure and solvation structure in a self-consistent manner.

Recently, we studied the bond formation step 1 using RISM-SCF-SEDD.[12] We have clarified that the solvation effect governs the free energy profile. The interplay between the hydration around the oxygen of CO_2 and the dehydration around the nitrogen is essential for the mechanism of the bond formation. A solvation effect is considered to be also crucial in the second step (i.e., proton transfer), but the role of solvent is still unclear. Only few studies based on the dielectric continuum model and cluster model just considering a few water molecules nearby have been reported so far.[13−15] In this study, we would like to accomplish a full understanding of the chemical absorption of CO_2 by MEA using RISM-SCF-SEDD, especially focusing on the proton transfer step.

METHOD

Here we briefly summarize RISM-SCF-SEDD. A more detailed explanation of the theory can be found in the previous articles.[7−11] RISM-SCF-SEDD utilizes one-dimensional RISM theory to treat solvent. The main equation is as follows.[10,11]

$$\mathbf{h} = \boldsymbol{\omega}^*\mathbf{c}^*\boldsymbol{\omega} + \boldsymbol{\omega}^*\mathbf{c}^*\boldsymbol{\rho}\mathbf{h} \quad (3)$$

Received: December 19, 2011
Revised: January 25, 2012
Published: February 10, 2012

where '*' denotes a convolution integral, and all the quantities are matrices whose element corresponds to a pair of interaction sites; $\boldsymbol{\rho}$ is the number of density; and $\boldsymbol{\omega}$ is the intramolecular correlation function defining the molecular geometry. In eq 3, **h** (total correlation function) and **c** (direct correlation function) are unknown functions to be solved. Hyper-netted chain (HNC) closure is a well-known equation to be coupled with the equation

$$c_{\alpha s}(r) = \exp[-\beta u_{\alpha s}(r) + \gamma_{\alpha s}(r)] - \gamma_{\alpha s}(r) - 1$$
$$\gamma_{\alpha s}(r) = h_{\alpha s}(r) - c_{\alpha s}(r) \quad (4)$$

where α and s are, respectively, solute and solvent site; $u_{\alpha s}(r)$ is interaction potential between them; and $\beta = 1/k_B T$. Solvation free energy ($\Delta\mu$) is readily evaluated by $h_{\alpha s}(r)$ and $c_{\alpha s}(r)$ with an HNC formula[16]

$$\Delta\mu^{\mathrm{HNC}} = -\frac{1}{\beta}\sum_{\alpha,s}\int d\mathbf{r}\rho_s\left[c_{\alpha s}(r) - \frac{1}{2}h_{\alpha s}^2(r) + \frac{1}{2}h_{\alpha s}(r)c_{\alpha s}(r)\right] \quad (5)$$

or with the Gaussian fluctuation (GF) formula[17]

$$\Delta\mu^{\mathrm{GF}} = -\frac{1}{\beta}\sum_{\alpha,s}\int d\mathbf{r}\rho_s\left[c_{\alpha s}(r) + \frac{1}{2}h_{\alpha s}(r)c_{\alpha s}(r)\right] \quad (6)$$

The GF evaluation (eq 6) often shows better agreement with experimental result than the HNC evaluation (eq 5), though the physical background of the HNC formula is considered to be clearer. More accurate free energy calculation methods based on RISM theory have been recently developed, and the extensive studies with these methods also show that the GF evaluation provides better agreement than the HNC evaluation.[18−22]

Total free energy of the system with RISM-SCF-SEDD is defined as

$$\mathcal{A} = E_{\mathrm{solute}} + \Delta\mu \quad (7)$$

where E_{solute} is the total energy of the solute molecule described by a standard ab initio molecular orbital theory and $\Delta\mu$ is given by eq 5 or 6. The change of free energy caused by solvation is given by

$$\Delta\mathcal{A} = \mathcal{A} - E_{\mathrm{gas}} = E_{\mathrm{reog}} + \Delta\mu \quad (8)$$

where E_{reog} is the energy difference of the solute molecule from its isolated state (E_{gas}) upon the solvation.

$$E_{\mathrm{reog}} \equiv E_{\mathrm{solute}} - E_{\mathrm{gas}} = \langle\Phi|H|\Phi\rangle - \langle\Phi_0|H|\Phi_0\rangle \quad (9)$$

Here $|\Phi\rangle$ and $|\Phi_0\rangle$ are wave functions in the solution phase and in the gas phase, respectively.

COMPUTATIONAL DETAILS

Geometry optimizations were carried out with B3LYP/6-311++G** under the restriction of C_s symmetry, in which CO_2 and N−C−C−O−H are in the same plane. Energy calculations were then performed with CCSD(T)/6-311++G** at the obtained geometry. PCM[23] computation was also performed for comparison purposes. The RISM equation was solved with hyper-netted chain (HNC) closure.[16] The Lennard-Jones parameters of the solute were taken from refs 24−27, and SPC-like water[28] was employed for the solvent. All of them are summarized in Table 1.

Table 1. Lennard-Jones Parameters

	σ/Å	ε/kcal mol^{-1}
	Solute	
N	3.300	0.170
C(methyl)	3.500	0.066
C(CO_2)	3.296	0.120
O(OH)	3.070	0.170
O(CO_2)	2.850	0.200
H(methyl)	2.500	0.030
H(HO)	1.000	0.0560
	Solvent	
O	3.166	0.1550
H	1.000	0.0560

The resonance structure analysis developed by us was employed.[29] Pipek−Mezey localization[30] was utilized to separate valence orbitals, and the weight of resonance structure is evaluated with the standard Löwdin-type operator. Unfortunately, the π orbital and the lone-pair orbital in the carbon dioxide moiety were mixed together. These two orbitals were thus chosen to evaluate the weight of the C−O bond, and then the contribution from lone-pair orbitals corresponding to C^+O^- was subtracted to evaluate the resonance structure.[12]

Geometry optimizations in gas-phase and PCM computations were carried out by the Gaussian 03 program.[31] All other computations were performed with GAMESS package,[32] in which our developed methods were implemented.

RESULTS AND DISCUSSION

Reaction Profile. The reaction profile is shown in Scheme 1. The geometry optimization in aqueous solution is performed for the step 1 in this study, and the obtained energy profile is mostly the same as that in the previous one.[12] **2** is an intermediate before the bond formation between CO_2 carbon (C_{cdx}) and the nitrogen. After passing through the transition state ($\mathbf{TS_{2-3}}$), another intermediate **3** is produced.

The proton transfer step proceeds from **3**, and three paths are possible. In the first path, H_2O acts as the base, then **4** and H_3O^+ (**5a**) are yielded. If another **1a** (MEA) acts as the base, **4** and the protonated MEA (**5b**) are produced (the second path). The third path is an intramolecular proton transfer from the nitrogen moiety to CO_2 oxygen (O_{cdx}) to form **6**. Although **6** has not been observed in experimental studies, an ab initio electronic structure calculation of the water-cluster model reported that **6** is stable.[14]

An anion (**4**) is produced in both the first and second paths. As expected, this species is notably affected by solvation, and the geometry in aqueous solution is substantially different from the gas phase one. For example, the O_{cdx}−C_{cdx}−O_{cdx} bond angle is changed from 131° (gas phase) to 124° (aqueous solution). The decrease of the angle should be related to the change in the electronic structure of the CO_2 moiety. As shown in the previous study, the double bond character is reduced when the N−C bond is formed. The π conjugation in CO_2 is suppressed, and the electron tends to be isolated at oxygen atoms. In other words, the electron is shifted from the nitrogen lone pair to the CO_2 π^* orbital. The further bending in aqueous solution thus indicates that the solvation promotes the occupation of the π^* orbital. In fact, the natural charge on

dx.doi.org/10.1021/jp212225r | J. Phys. Chem. B 2012, 116, 2244−2248

Scheme 1. Reaction Scheme of MEA and CO_2[a]

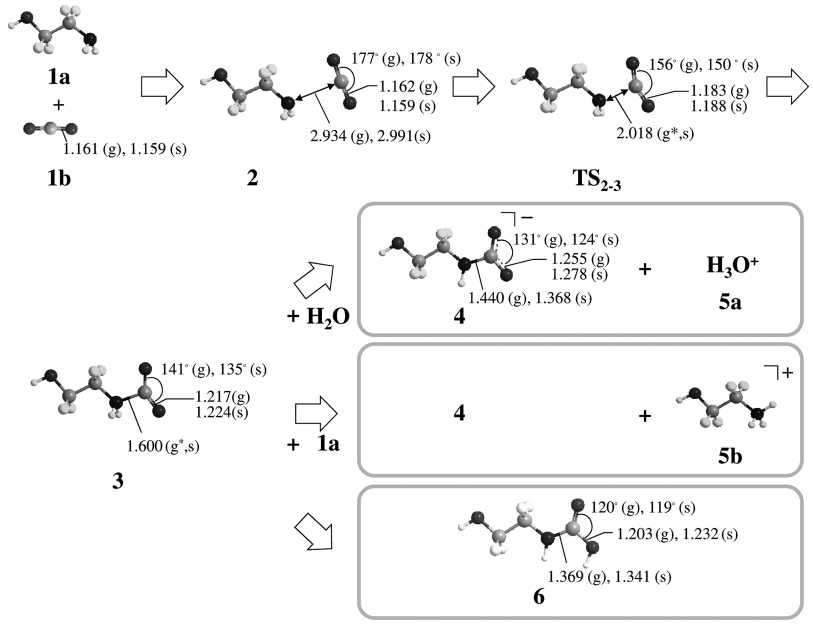

[a]Bond lengths of C_{cdx}–N and C_{cdx}–O in Å and the bond angle of O_{cdx}–C_{cdx}–O_{cdx} are shown. (g) and (s) mean that the structure is optimized in the gas phase and in aqueous solution with RISM-SCF-SEDD, respectively. Since TS_{2-3} and **3** are nonexistent in the gas phase (marked with '*'), the C_{cdx}–N bond length is fixed to that in aqueous solution, and all other degrees of freedom were optimized.

the CO_2 moiety decreases from −0.73 lel (gas phase) to −0.92 lel (aqueous solution), and the C_{cdx}–O_{cdx} bond is lengthened. The bond length of C_{cdx}–N is also noticeably changed from 1.440 Å (gas phase) to 1.368 Å (aqueous solution). These geometry changes clearly indicate that solvation considerably affects the electronic structure. As shown below, this is deeply related to the strong hydration of the O_{cdx} site. In a different standpoint, the bond polarization in C_{cdx}–O_{cdx} by the solvation enhances the drawing of electron from MEA to CO_2.

Free Energy Profile. The free energy profile along the reaction is shown in Figure 1. First, we briefly summarize the bond formation step. For the reaction in aqueous environment, both free energy profiles evaluated by HNC and GF methods are presented. In the gas phase, the potential energy is monotonically increased after the formation of the intermediate (**2**). However, in aqueous solution, the transition state (TS_{2-3}) and an intermediate (**3**) are found. By analyzing the pair correlation functions (PCFs), it was revealed that the development of hydrogen bonding around O_{cdx} and dehydration around nitrogen are virtually canceled out near the transition state, although the energy curve looks very similar to that in the gas phase.[12] The hydration of O_{cdx} then gradually becomes dominative to form stable **3**. In other words, the bond formation step is understood as an interplay between the solvation around O_{cdx} and the desolvation around the nitrogen.[12]

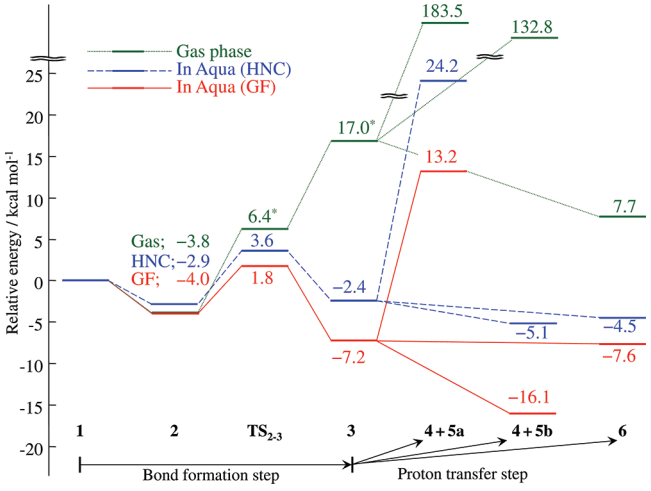

Figure 1. Total potential energy profile in the gas phase (green dotted line) and free energy profile in aqueous solution calculated by RISM-SCF-SEDD using HNC (blue dashed line) and GF (red solid line). Concerning the '*' mark, see Scheme 1.

Let us then focus on the proton transfer step, which is the main subject of the present study. Among the three paths, the energy of the first path to give **4** + **5a**, in which H_2O acts as the base, is very high in the gas phase (+183.5 kcal mol^{-1}). Although this is dramatically stabilized in aqueous solution, the total free energy is still positive, +24.2 kcal mol^{-1} (HNC) and +13.2 kcal mol^{-1} (GF). For the second path, the reaction energy in the gas phase is lower than the first path by about 50 kcal mol^{-1} due to the stronger basicity of **1a** (MEA) than H_2O,[33] but the final product is still very unstable (+132.8 kcal mol^{-1}). However, the total free energy of **4** + **5b** in aqueous solution is definitely negative (−5.1 kcal mol^{-1} by HNC and −16.1 kcal mol^{-1} by GF), and the transfer becomes exothermic. Both of the formulas clearly show that **4** + **5b** is more stable, indicating that MEA (**1a**) acts as the base in reality. **6** is much more stable than **4** + **5a** or **4** + **5b** in the gas phase, but the contribution from solvation is rather small. Consequently, **6** is slightly unstable compared to **4** + **5b** in an aqueous environment, but the difference between them is only 0.6 kcal mol^{-1} by HNC and 8.5 kcal mol^{-1} by GF. The result suggests that the intramolecular proton transfer could occur to produce **6**, but the transferred proton is eventually abstracted by MEA. The details of the mechanism might be further

dx.doi.org/10.1021/jp212225r | J. Phys. Chem. B 2012, 116, 2244–2248

clarified, for example, by changing the chemical composition of MEA (**1a**) in an experiment. In any of these cases, H_2O does not act as the base. It should be emphasized that it is the solvation effect that mainly determines the relative stability of the final products.

The change of solvation structure reveals the role of solvation at the molecular level. Figure 2 shows PCFs between O_{cdx} to

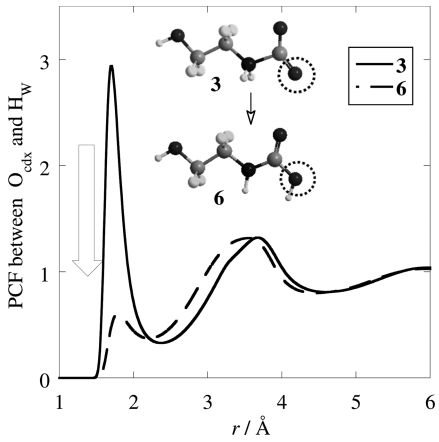

Figure 2. PCF between O_{cdx}–H_W of **3** (solid line) and **6** (dashed line).

which the proton transfers, and water hydrogen (H_W) in **3** and **6**. The sharp peak at $r \simeq 2$ Å in **3** corresponds to the hydrogen bond, showing the strong interaction before the intramolecular transfer. The peak height is significantly decreased from 2.9 to 0.6 by completing the transfer. Actually, the desolvation around O_{cdx} is consistent with the increase of $\Delta\mathcal{A}$ from **3** to **6**. In other words, the solvation slightly prevents the protonation of O_{cdx} in **3**.

Origin of the Stabilization of Final Products. Since the remarkable stabilization of **4** + **5b** by solvation is the origin of the exothermicity of the reaction, solvation energy is further analyzed. Hereafter, we discuss mainly the GF evaluation for brevity, but the HNC evaluations give qualitatively the same results. The great stabilization of the final product obtained by the present computation is consistent with experimental knowledge. Figure 3 displays $\Delta\mathcal{A}$ of the possible products of

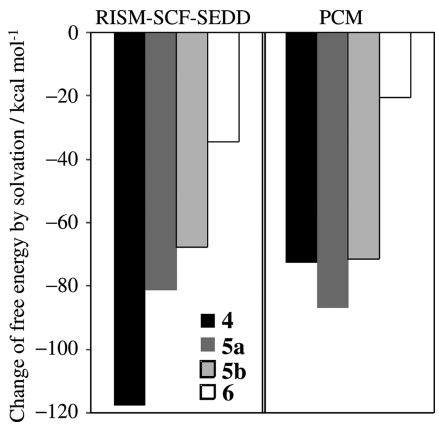

Figure 3. Change of free energy by solvation ($\Delta\mathcal{A}$) computed by RISM-SCF-SEDD (left) and PCM (right).

the reaction computed by RISM-SCF-SEDD as well as by PCM. Both RISM-SCF-SEDD and PCM computations show a similar trend as a whole, but the difference in **4** is remarkable. $\Delta\mathcal{A}$ by RISM-SCF-SEDD (-117.6 kcal mol^{-1}) is noticeably lower than the other species (**5a**: -81.4 kcal mol^{-1}, **5b**: -67.9 kcal mol^{-1}, **6**: -34.6 kcal mol^{-1}). Note that $\Delta\mathcal{A}$ with the HNC evaluation is also lower than those of the other species. This distinct stabilization of **4** is the main source of the exothermicity of the reaction. This result may be interesting from the viewpoint of conventional solution chemistry because solvation free energy of the same-charged species is generally in inverse proportion to the radius of species according to the dielectric continuum theory.[34] In fact, as shown in Figure 3, $\Delta\mathcal{A}$ of **4** evaluated with PCM (-72.6 kcal mol^{-1}) is similar to that of **5b** (-71.3 kcal mol^{-1}) and higher than that of **5a** (H_3O^+) with a small volume (-86.9 kcal mol^{-1}).

The stabilization of **4** with RISM-SCF-SEDD thus comes from the solute–solvent specific interaction at the molecular level, which is not adequately described by the dielectric continuum model. The origin may be further analyzed by "formally" dividing $\Delta\mu^{GF}$ (eq 6) into the contribution from each atom labeled α.

$$\Delta\mu_\alpha^{GF} = -\frac{1}{\beta}\sum_s \int d\mathbf{r}\rho_s\left[c_{\alpha s}(r) + \frac{1}{2}h_{\alpha s}(r)c_{\alpha s}(r)\right] \quad (10)$$

As expected, the contribution from the CO_2 moiety is dominative (-102.2 kcal mol^{-1}), corresponding to 87% of the total stabilization. Further decomposition reveals that the solvation around O_{cdx} is essential to understand the stabilization. Figure 4 illustrates the change of solvation

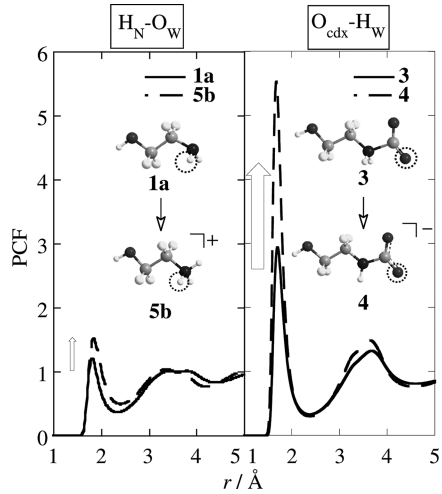

Figure 4. PCFs between H_N and O_W (left-hand side) and between O_{cdx} and H_W (right-hand side) before (solid line) and after (dashed line) the proton transfer.

structure around O_{cdx} and hydrogen in the amino moiety (H_N) that makes another hydrogen bond with solvent water. Both of them correspond to a change from a neutral species to a charged one; from **1a** (MEA) to **5b** (left-hand side) and from **3** to **4** (right-hand side). The peak at $r \simeq 2$ Å of PCFs between H_N and water oxygen (O_W) is obviously a hydrogen bond, which remains mostly unchanged on the proton transfer (**1a** → **5b**). In contrast, the peak corresponding to the hydrogen bond ($r \simeq 2$ Å) between O_{cdx} and water hydrogen (H_W) becomes much higher through the transfer, and the height increases from 3.0 (**3**) to 5.5 (**4**). This dramatic change of hydration is a key to understanding the stability of **4** and the driving force of the promotion of the proton transfer.

dx.doi.org/10.1021/jp212225r | J. Phys. Chem. B 2012, 116, 2244–2248

The strength of the hydrogen bond may be interpreted using the resonance structures. Concerning the $N-H_N$ bond in **5b**, the covalent bond character ($N-H_N$) is the largest contribution (42%). However, the two ionic contributions are also considerably large ($N^-H_N^+$, 36%, and $N^+H_N^-$, 12%). In other words, the positive charge is not localized only on H_N but distributes over the whole NH_3 moiety. Accordingly, H_N does not strongly attract water oxygen (O_W). On the other hand, the ionic bond character ($C_{cdx}^+O_{cdx}^-$) is evidently dominant (62%) in the $C_{cdx}O_{cdx}$ moiety in **4**, whereas the covalent character ($C_{cdx}-O_{cdx}$) is not significant (28%). The electron (negative charge) is strongly localized at O_{cdx}, which causes the strong interaction with solvent water.

CONCLUSION

In this work, the reaction between MEA and CO_2 is investigated using the RISM-SCF-SEDD method, which deals with the solvation effect based on a molecular theory. It is shown that MEA acts as the base, and the following insights into the reaction are obtained.

In the bond formation step, the barrier height is determined by hydration around O_{cdx} in the CO_2 moiety and dehydration around the nitrogen. The hydration around O_{cdx} then significantly drives the stabilization of the final product. In other words, the solvation around O_{cdx} mainly controls the reaction of MEA and CO_2. The strong interaction between O_{cdx} and H_W could be understood by the dominative resonance character of $C_{cdx}^+O_{cdx}^-$. These insights might indicate that the solvation around O_{cdx} could be a key to designing a new efficient amine for CO_2 absorption.

AUTHOR INFORMATION

Corresponding Author

*E-mail: hirofumi@moleng.kyoto-u.ac.jp.

Notes

The authors declare no competing financial interest.

ACKNOWLEDGMENTS

We thank Drs. Atsushi Ikeda and Daisuke Yokogawa for proving the computational codes and Prof. Shigeyoshi Sakaki for valuable discussion. The work is financially supported in part by a Grant-in-Aid for Scientific Research on Priority Areas "Molecular Science for Supra Functional Systems" (477-22018016), Grant-in-Aid for Scientific Research on Innovative Areas "Molecular Science of Fluctuations" (2006-21107511), as well as by Grant-in-Aid for Scientific Research (C) (20550013). K.I. thanks the Grant-in-Aid for JSPS Fellows. The Strategic Programs for Innovative Research (SPIRE), the Computational Materials Science Initiative (CMSI), and the Ministry of Education, Culture, Sports, Science and Technology (MEXT), Japan, are also acknowledged.

The authors also thank Dr. Yukihiko Inoue for drawing their attention to the importance of this subject.

REFERENCES

(1) Vaidya, P. D.; Kenig, E. Y. *Chem. Eng. Technol.* **2007**, *30*, 1467.
(2) Alper, E. *Ind. Eng. Chem. Res.* **1990**, *29*, 1725.
(3) Hikita, H.; Asai, S.; Ishikawa, H.; Honda, M. *Chem. Eng. J.* **1977**, *13*, 7.
(4) Crooks, J. E.; Donnellan, J. P. *J. Chem. Soc., Perkin Trans. 2* **1989**, *4*, 331.
(5) Ali, S. H. *Int. J. Chem. Kinet* **2005**, *37*, 391.
(6) Bonenfant, D.; Mimeault, M.; Hausler, R. *Ind. Eng. Chem. Res.* **2003**, *42*, 3179.
(7) Yokogawa, D.; Sato, H.; Sakaki, S. *J. Chem. Phys.* **2007**, *126*, 244504.
(8) Ten-no, S.; Hirata, F.; Kato, S. *J. Chem. Phys.* **1994**, *100*, 7443.
(9) Sato, H.; Hirata, F.; Kato, S. *J. Chem. Phys.* **1996**, *105*, 1546.
(10) Andersen, H. C.; Chandler, D. *J. Chem. Phys.* **1972**, *57*, 1930.
(11) Hirata, F.; Rossky, P. J. *Chem. Phys. Lett.* **1981**, *83*, 329.
(12) Iida, K.; Yokogawa, D.; Ikeda, A.; Sato, H.; Sakaki, S. *Phys. Chem. Chem. Phys.* **2009**, *11*, 8556.
(13) da Silva, E. F.; Svendsen, H. F. *Ind. Eng. Chem. Res.* **2004**, *43*, 3413.
(14) Arstad, B.; Blom, R.; Swang, O. *J. Phys. Chem. A* **2007**, *111*, 1222.
(15) Shim, J.-G.; Kim, J.-H.; Jhon, Y. H.; Kim, J.; Cho, K.-H. *Ind. Eng. Chem. Res.* **2009**, *48*, 2172.
(16) Singer, S. J.; Chandler, D. *Mol. Phys.* **1985**, *55*, 621.
(17) Chandler, D.; Singh, Y.; Richardson, D. M. *J. Chem. Phys.* **1984**, *81*, 1975.
(18) Ratkova, E. L.; Chuev, G. N.; Sergiievskyi, V. P.; Fedorov, M. V. *J. Phys. Chem. B* **2010**, *114*, 12068.
(19) Karino, Y.; Fedorov, M. V.; Matubayasi, N. *Chem. Phys. Lett.* **2010**, *496*, 351.
(20) Frolov, A. I.; Ratkova, E. L.; Palmer, D. S.; Fedorov, M. V. *J. Phys. Chem. B* **2011**, *115*, 6011.
(21) Palmer, D. S.; Sergiievskyi, V. P.; Jensen, F.; Fedorov, M. V. *J. Chem. Phys.* **2010**, *133*, 044104.
(22) Ten-no, S. *J. Chem. Phys.* **2001**, *115*, 3724.
(23) Tomasi, J.; Mennucci, B.; Cammi, R. *Chem. Rev.* **2005**, *105*, 2999.
(24) Rizzo, R. C.; Jorgensen, W. L. *J. Am. Chem. Soc.* **1999**, *121*, 4827.
(25) Jorgensen, W. L. *J. Phys. Chem.* **1986**, *90*, 1276.
(26) Weiner, S. J.; Kollman, P. A.; Case, D. A.; Singh, U. C.; Ghio, C.; Alagona, G.; Profeta, S.; Weiner, P. *J. Am. Chem. Soc.* **1984**, *106*, 765.
(27) Weiner, S. J.; Kollman, P. A.; Nguyen, D. T.; Case, D. A. *J. Comput. Chem.* **1986**, *7*, 230.
(28) Berendsen, H. J. C.; Postma, J. P. M.; van Gunsteren, W. F.; Hermans, J. In *Intermolecular Forces*; Pullman, B., Ed.; Reidel: Dordrecht, 1981.
(29) (a) Ikeda, A.; Nakao, Y.; Sato, H.; Sakaki, S. *J. Phys. Chem. A* **2006**, *110*, 9028. (b) Ikeda, A.; Yokogawa, D.; Sato, H.; Sakaki, S. *Chem. Phys. Lett.* **2006**, *424*, 499. (c) Ikeda, A.; Yokogawa, D.; Sato, H.; Sakaki, S. *Int. J. Quantum Chem.* **2007**, *107*, 3132. (d) Ikeda, A.; Nakao, Y.; Sato, H.; Sakaki, S. *J. Chem. Theory Comput.* **2009**, *5*, 1741. (e) Ikeda, A.; Nakao, Y.; Sato, H.; Sakaki, S. *Chem. Phys. Lett.* **2011**, *505*, 148.
(30) Pipek, J.; Mezey, P. G. *J. Chem. Phys.* **1989**, *90*, 4916.
(31) *Gaussian 03*, Revision C.02; Gaussian Inc.: Wallingford, CT, 2004.
(32) Schmidt, M. W.; Baldridge, K. K.; Boatz, J. A.; Elbert, S. T.; Gordon, M. S.; Jensen, J. H.; Koseki, S.; Matsunaga, N.; Nguyen, K. A.; Su, S.; Windus, T. L.; Dupuis, M.; Montgomery, J. A. *J. Comput. Chem.* **1993**, *14*, 1347.
(33) Perrin, D. D. *Dissociation constants of organic bases in aqueous solution*; London: Butterworths, 1972.
(34) Bottcher, C. J. F. *Theory of Electric Polarization*; Elsevier: Amsterdam, 1983.